

Experimental Upper Limit for the Permanent Electric Dipole Moment of Rb^{85} by Optical-Pumping Techniques*†

E. S. ENSBERG‡

University of Washington, Seattle, Washington

(Received 25 July 1966)

An optical-pumping experiment designed to detect a permanent electric dipole moment in the ground state of the Rb^{85} atom is described. It has the advantage of averaging out the motional magnetic fields that limit the more recent related atomic-beam results. The applied electric fields were necessarily smaller. Zeeman transitions in free Rb^{85} atoms in the earth's magnetic field (about 210 kc/sec) were observed in evacuated, wall-coated absorption cells under electric fields up to ± 2000 V/cm. Modulation of the light beam by precessing atoms was used to operate the samples as self-excited oscillators. The difference in frequency between two Rb^{85} oscillators operating side by side in the same light beam was measured to reduce the effect of magnetic field fluctuations. This frequency difference (about 300 cps) was found to be stable to within ± 0.1 cps (e.g., corresponding to magnetic-field variations between samples of 2×10^{-7} G for 30-min periods, under favorable conditions), and was found to be independent of the electric field applied to one of them within that limit. It was concluded that the permanent electric dipole moment of the Rb^{85} atomic ground state, if it exists, is less than $e \times (10^{-18} \text{ cm})$, where e is the electronic charge. The theory of optically pumped alkali oscillators is developed for arbitrary nuclear spin in the limit of low light intensities (the high-resolution case).

INTRODUCTION

AS previously reported,¹ this experiment set an upper limit for the permanent electric dipole moment of the Rb^{85} atom of about 10^{-18} cm times the electronic charge e . Since then, similar experiments in atomic beams have set a limit for Cs^{133} which is lower by about a factor of 10.^{2,3} Possible implications of this experiment as a test of time-reversal invariance have been discussed by Sachs and Schwebel⁴ and by Sandars,³ whose calculation for the heavy alkalis indicates that these results imply much lower limits on the permanent electric dipole moment of the free electron.

Optical-pumping and beam methods have quite different limitations. "Motional" magnetic fields³ (of the form $\mathbf{v} \times \mathbf{E}$ for atomic velocity \mathbf{v} and applied electric field \mathbf{E}) are averaged out and resonance lines are much narrower in optical pumping, but electric fields are limited by larger electrode spacings and delicate cell linings. In both methods the linear Stark effect would have been observed as a small perturbation on the alkali ground-state Zeeman splitting.

In this experiment, circularly polarized resonance radiation (7947.6 Å " D_1 " line) polarized⁵ a vapor of

rubidium atoms in an evacuated absorption cell. The modulation of the transmitted light beam at the Larmor frequency drove the resonance through a feedback loop, forming the type of self-driven oscillator suggested by Dehmelt.^{6,7} The beat frequency between a pair of such oscillators proved independent of relatively large fluctuations in ambient magnetic field and was therefore a sensitive detector of frequency shifts caused by an electric field applied to one of them.

APPARATUS

The light beam for both oscillators was provided by a single Varian spectral lamp (Fig. 1) powered by a regulated current supply. Given proper warm-up and environment, it proved very stable and free of noise. It was mounted about 12 in. from the two absorption cells and directed at a point between them. A 3-in. commercial dielectric filter, with a bandpass of 80 Å approximately centered at 7947.6 Å, was used to select D_1 radiation. The ratio of the transmittances of D_1 to D_2 intensities varied from about 500 at normal incidence to about 95 at 12° , the maximum angle at which light reached the samples in the experiment. Sheet polarizers and retardation sheets were selected to transmit about 90% circularly polarized light at normal incidence.

An evacuated absorption cell was essential for the application of strong electric fields. Spin relaxation at the walls of the evacuated cell was reduced by the technique of coating them with wax, according to the method now generally used, first employed by Robinson, Ensberg, and Dehmelt.⁸ In this case, dotriacontaine

* Submitted as a thesis in partial fulfillment of the requirements for the degree of Doctor of Philosophy at the University of Washington.

† Supported by contracts and/or grants from the Army Research Office (Durham), the Office of Naval Research, and the National Science Foundation. Preparation of this paper was partly accomplished at Yale University with the support of the Air Force Office of Scientific Research.

‡ Present address: Physics Department, Yale University, New Haven, Connecticut.

¹ E. S. Ensberg, *Bull. Am. Phys. Soc.* **7**, 534 (1962).

² E. Lipworth and P. G. H. Sandars, *Phys. Rev. Letters* **13**, 716 (1964).

³ P. G. H. Sandars and E. Lipworth, *Phys. Rev. Letters* **13**, 718 (1964).

⁴ M. Sachs and S. L. Schwebel, *Ann. Phys. (N.Y.)* **8**, 475 (1959).

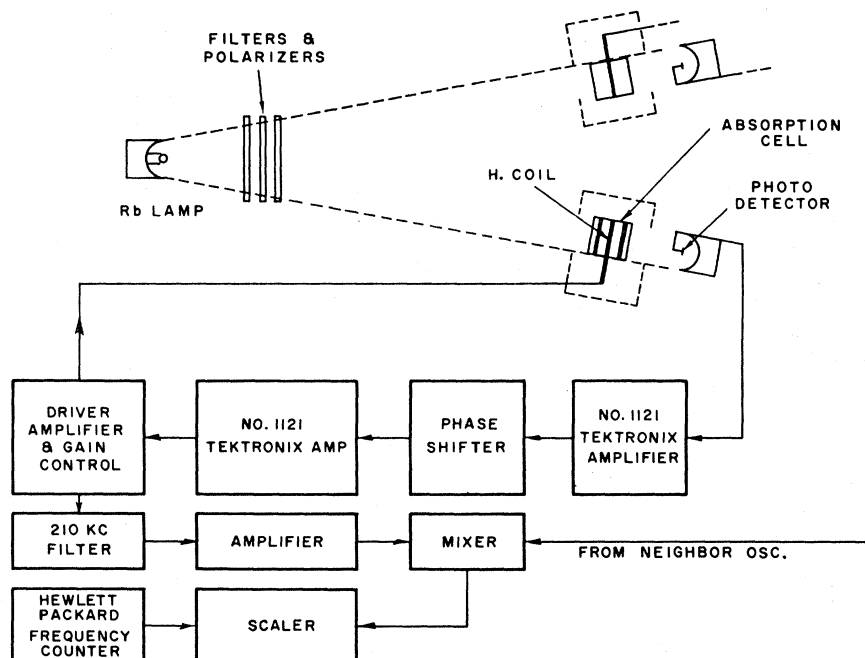
⁵ A. Kastler, *Proc. Phys. Soc. (London)* **A67**, 853 (1954); *J. Opt. Soc. Am.* **47**, 460 (1957).

⁶ H. G. Dehmelt, *Phys. Rev.* **105**, 1924 (1957).

⁷ A. L. Bloom, *Appl. Opt.* **1**, 61 (1962).

⁸ H. G. Robinson, E. S. Ensberg, and H. G. Dehmelt, *Bull. Am. Phys. Soc.* **3**, 9 (1958); D. Kleppner, N. F. Ramsey, and P. Fjelstad, *Phys. Rev. Letters* **1**, 232 (1958); H. M. Goldenberg, D. Kleppner, and N. F. Ramsey, *Phys. Rev.* **123**, 530 (1961).

FIG. 1. Two rubidium samples were illuminated by the same spectral lamp. The block diagram of the feedback loop for the sample with Stark electrodes is shown. Its neighbor had an identical feedback loop, whose output is indicated here as an input to the mixer.



(C₃₂H₆₆) was used. The absorption cells used in this experiment were Pyrex cylinders about 28 mm long and 28 mm in outside diameter (Fig. 2). The measured longitudinal relaxation time of 0.1 sec suggests that the rubidium atoms bounced at least 1400 times off these walls before losing their spin orientation. Metallic rubidium in a side tube supplied the vapor which reached the absorption cell through an aperture in the wall with a diameter of 3/4 mm. A simple glass ionization pump was installed on each sample to ensure good vacuum for the life of the samples.

Another advantage of an evacuated cell is the reduction of the field-inhomogeneity contribution to line breadth. If the order of magnitude of this "motional narrowing" is estimated by the usual random-walk argument,⁹ a gradient corresponding to a linewidth $\Delta\nu$ for stationary atoms gives an effective linewidth $\delta\nu \approx (\Delta\nu)^2/\Omega$, where Ω is the "rattle frequency" of the atoms at thermal velocities in the evacuated sample. In this case, typical numbers are $\Omega = 10^4$ cps, $\Delta\nu = 700$ cps, or $\delta\nu \approx 50$ cps.

Three sets of simple gradient-reducing coils sufficed to reduce the linewidth by only another factor of 2. (In practice, to prevent the accidental phase-locking of the oscillators to each other through stray H_1 fields, the gradient was never reduced to zero.)

In order to apply Stark fields to one of the samples, a heavy (incomplete) ring of silver paint was baked on the outside wall of the sample near each end. The potential of these rings was varied symmetrically with respect to ground so the mid-plane of the cell was normally at

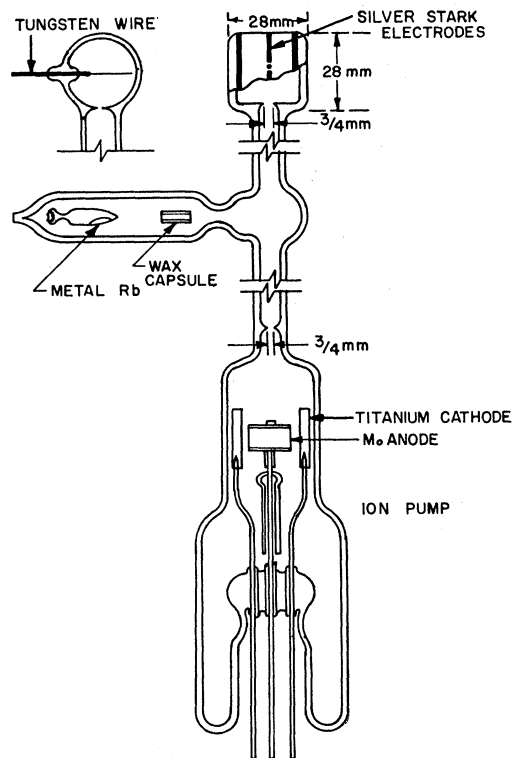


FIG. 2. A rubidium sample. The electrometer wire shown at top left was used to measure the internal electric field. The wax was pre-distilled at low temperatures and pushed into the neck of the sample in an open capsule during construction. After evacuation, a drop of the melted wax was forced through the aperture by inert gas. The ion pump (Penning pump) was rarely used after ensuring good vacuum in the completed sample.

⁹ D. Pines and C. P. Slichter, Phys. Rev. **100**, 1014 (1955).

ground potential. Because of the highly insulating interior wax walls, a simple electrometer was sealed into the sample to test the strength of the internal electric field. This electrometer consisted of a fine tungsten wire extending through the glass wall, whose deflection in the field could be measured as a function of its own potential. The deflection was observed before and after evacuation and wall-coating of the absorption cell and was found to be identical with the deflection of a comparable wire suspended in open air between mockup electrodes approximating the shape of the silver-paint rings. Rb^{85} disorientation by the wire was negligible because its surface was small compared with the aperture in the glass wall.

The samples were mounted in the light beam on an optical bench which was tilted to make an angle of about 45° with respect to the earth's magnetic field. At this angle, the single light beam can both produce an atomic polarization and be modulated at the Larmor frequency.

Positioned behind each absorption cell, in the transmitted beam, was a solid-state photodetector. The solid-state photovoltaic diode was used because of its large quantum efficiency at this wavelength. Its large internal capacitance necessitated the use of a small photosensitive area. Light was collected from the transmitted beam by a parabolic mirror, focused on the detector. A pair of matched gallium-arsenide-type GAU-401 (Philco) detectors were finally used, with an active area of 4 mm^2 and internal impedance of $3 \times 10^4 \Omega$ (at 0 V) and 160 pF shunt capacitance at 210 kc/sec. The dc photocurrent was measured directly with chopper-stabilized millimicro-ammeters. The rf modulation on the photocurrent was measured at the output of appropriate low-noise, wide-band preamplifiers. The noise of the preamplifiers, thermal noise of the detectors, and shot noise of the light beam were all of comparable magnitude. Raising the light intensity to increase the photocurrent from zero to $3 \mu\text{A}$ increased the noise voltage output by about 20%. A battery-operated incandescent flashlight bulb demonstrated the same order of magnitude of noise as this spectral lamp.

The resonant magnetic field was provided by single-turn " H_1 coils" rigidly supported around each sample by polystyrene cylinders to which they were cemented. Aluminum-foil-covered plywood boxes around each sample region were used to reduce the effect of each sample's H_1 field at its neighbor's site.

Cathode followers coupled the output from each preamplifier to a mixer through tunable filters which restricted the output to a 3-kc/sec band centered on the oscillator frequency. After additional amplification, the two outputs were mixed and the difference in their frequencies (determined mainly by the field gradient over the sample region) was mixed with the output of a stable laboratory oscillator. The resulting low-frequency (about 1 cps) beat was displayed by a pen recorder.

Since long observation times were required, this method of taking data was abandoned after it had been established that the system operated reliably. The alternative system of measuring frequency shifts involved counting the frequency in the output of the first mixer directly with a scaler. The counting time for a given number (usually 2×10^4 to 10^5) of cycles was measured against the frequency standard in the Hewlett Packard Model 524D frequency counter.

ABSORPTION PROBABILITIES

The theories of related optical-pumping experiments¹⁰⁻¹² grow complicated for large nuclear spin. In this experiment, high resolution requires low light intensity, permitting considerable simplification in the problem of expressing the connection between the Stark shift and the oscillation frequency of the rubidium oscillator. It is also assumed that the samples were optically thin and that equal optical intensities were available for all hyperfine components of the D_1 line.

Alkali atoms with nuclear and total angular momentum quantum numbers I and F , respectively, can have a total of only $4F_+$ Zeeman sublevels (Fig. 3) in their two ground-state hyperfine levels, where $F = I \pm \frac{1}{2}$ and F_+ is defined here as $I + \frac{1}{2}$. If there are n_k atoms in the k th sublevel, the total number of atoms in the cell is $\sum_k n_k = N$. The effect of the pumping radiation is to remove an atom from the k th sublevel to an excited state by absorption of a photon (with a change of magnetic quantum number m_k determined by the light beam polarization to be, for example, $+1$), from which it rapidly returns by spontaneous emission ($\Delta m = \pm 1, 0$) to another ground-state sublevel j . Given the probability per unit time $\beta_0 B_{jk}$ for this two-step transition between ground states, where β_0 = the absorption rate per atom

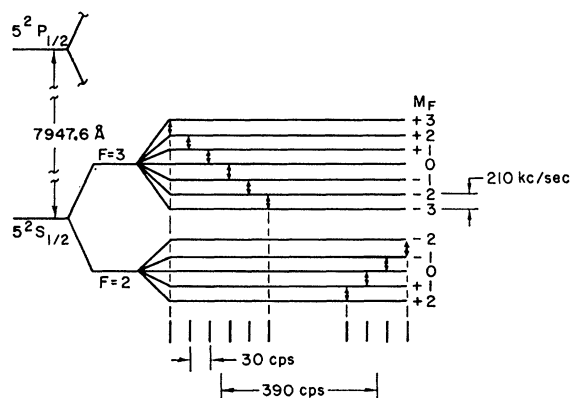


FIG. 3. Rb^{85} ground-state energy levels and transition frequencies at 0.47 G.

¹⁰ W. E. Bell and A. L. Bloom, Phys. Rev. **107**, 1559 (1957).

¹¹ J. N. Dodd and G. W. Series, Proc. Roy. Soc. (London) **A263**, 353 (1961).

¹² J. P. Barrat and C. Cohen-Tannoudji, J. Phys. Radium **22**, 329 (1961).

in the unpolarized vapor, one can compute the buildup of atomic polarization in the sample in the absence of relaxation.

It is then customary¹³ to write the absorption rate per atom β ,

$$\beta = \frac{\beta_0}{N} \sum_{k,j} B_{jk} n_k. \quad (1)$$

In the unpolarized vapor, $n_m \rightarrow N/4F_+$, $\beta \rightarrow \beta_0$, and

$$\sum_{kj} B_{jk} = 4F_+. \quad (2)$$

Certain other relationships between the B_{jk} 's can be calculated for an alkali with any I by simply performing the indicated sums¹⁴:

$$\sum_i B_{jk} = 1 \mp m_k / F_+, \quad (3)$$

$$\sum_i B_{kj} = 1 + \left[\frac{4F_+ \mp (F_+^2 + 2)}{3F_+^3} \right] m_k, \quad (4)$$

$$\sum_j B_{kj} - B_{jk} = \frac{2}{3F_+^3} [2F_+ \pm (F_+^2 - 1)] m_k, \quad (5)$$

where the upper sign is used if k designates a level for which $F = I + \frac{1}{2}$, the lower if $F = I - \frac{1}{2}$.

Using (3), for example,

$$\beta = \beta_0 \left[1 - \sum_k \pm \frac{m_k n_k}{F_+ N} \right].$$

Since the projection of the electron angular momentum on the axis defined by the light beam is proportional to $+m_k$ if $F = I + \frac{1}{2}$ and to $-m_k$ if $F = I - \frac{1}{2}$, the quantity

$$P_e \equiv \sum_k \pm \frac{m_k n_k}{F_+ N} \quad (6)$$

is just the electron polarization, and the absorption can be written

$$\beta = \beta_0 (1 - P_e). \quad (7)$$

This is a generalization of Dehmelt's result for the $I=0$ case.⁶ Equation (7) must be independent of any special choice of coordinate system; P_e is the instantaneous projection of the electron angular momentum on the light beam; β is the quantity actually measured in this experiment.

This absorption, in competition with various relaxation processes, is also responsible for establishing a polarization. For simplicity, assume all relaxation occurring by loss of polarized atoms and replacement of unpolarized atoms through the aperture in the cell wall. Then the characteristic relaxation time T_1 in all $4F_+$

sublevels would be equal and

$$\frac{dn_k}{dt} = \beta_0 \sum_i (B_{ki} n_i - B_{ik} n_k) + \frac{1}{T_1} \left(\frac{N}{4F_+} - n_k \right). \quad (8)$$

Equilibrium implies $dn_k/dt \rightarrow 0$ and the sublevel populations n_k are given by a set of coupled linear algebraic equations which have been numerically solved elsewhere for a number of special cases.^{13,15,16} An analytical solution has been performed, for $I = \frac{3}{2}$ only, by Raith.¹⁷

In weak light, however, the n_k are never far from their unpolarized values and Eq. (7) can be written in terms of their differences ϵ_k , expressed as fractions of the total population, defined by

$$n_k = N(1/4F_+ + \epsilon_k).$$

Then Eq. (8) becomes, to first order,

$$\frac{d\epsilon_k}{dt} \approx \frac{\beta_0}{4F_+} \sum_i (B_{ki} - B_{ik}) \epsilon_i - \frac{\epsilon_k}{T_1}. \quad (9)$$

Again, at equilibrium, $d\epsilon_k/dt \rightarrow 0$ and

$$\epsilon_k \rightarrow \epsilon_k^0 = \frac{\beta_0 T_1}{4F_+} \sum_i (B_{ki} - B_{ik}), \quad (10)$$

which, with (5) above, is

$$\epsilon_k^0 = \frac{\beta_0 T_1}{6F_+^4} [2F_+ \pm (F_+^2 - 1)] m_k. \quad (11)$$

The linear dependence on m_k suggests a Boltzmann distribution; the weakly polarizing light beam simply lowers the temperature of the spin system.

Also note that Eq. (11) predicts that the opposite ends of two hyperfine levels acquire increased populations for atoms with $I \geq \frac{5}{2}$. This effect in vacuum samples (no reorientation in the excited states) arises from competition between absorption and spontaneous-emission probabilities which can lead to "inverted-signal" effects similar to those recently described by Franz.¹⁶

In terms of the electron polarization, Eq. (9) becomes

$$\frac{dP_e}{dt} = \frac{P_e^0 - P_e}{T_1} \quad (12)$$

for any alkali atom as well as for the familiar spin $\frac{1}{2}$ ($I=0$) case, where

$$P_e^0 = \beta_0 T_1 \zeta \quad (13)$$

and

$$\zeta = \left[\frac{2F_+^4 + 5F_+^2 - 1}{9F_+^4} \right]. \quad (14)$$

Physically, the factor ζ is the change in electron polarization

¹³ W. Franzen and A. G. Emslie, Phys. Rev. **108**, 1453 (1957).

¹⁴ See Appendix.

¹⁵ B. Hawkins, Phys. Rev. **123**, 544 (1961).

¹⁶ F. A. Franz, Phys. Rev. **141**, 105 (1966).

¹⁷ W. Raith, Z. Physik **163**, 467 (1961).

tion per photon scattered by the unpolarized alkali vapor. For example, if $I=0$, then $\zeta=\frac{2}{9}$. That means that for three photons absorbed, one atom is transferred to the nonabsorbing state, increasing the polarization once for the state depleted and once for the state newly populated. For $I\rightarrow\infty$, ζ falls to $2/9$, not to zero as one might expect for a very large number of sublevels. The reason is, of course, that $\Delta F=+1$ transitions are allowed, resulting in occasional large fractional changes in electron polarization per photon.¹⁸

Since the magnetic moment of the alkali ground state is essentially that of the electron, the gyromagnetic ratio γ changes sign with the electron polarization; the macroscopic magnetic moment of the sample as a whole is then just $\gamma\hbar F_+NP_e=M_0$, where \hbar is Planck's constant divided by 2π . In the presence of a static, weak, homogeneous magnetic field parallel to the optical axis, the preceding results are unchanged.

In general, several complications arise when the light beam and magnetic field are not parallel or when a transverse monitoring beam is used.¹⁰⁻¹² In weak light, things are simpler. This is most easily seen by thinking of the light as a series of short pulses of a length consistent with the optical spectral width.¹⁹ For this lamp that width was probably Doppler breadth²⁰; in any case the interaction time is very short compared to a Larmor period, for example. Thus the magnetic field can be ignored during the time of interaction with any single optical pulse.

Each pulse contributes its increment of sample magnetization along the optical axis z' , making an angle θ with the magnetic field z (see Fig. 4). After the pulse, each increment of magnetization precesses away from the optical axis about the magnetic field or z axis. In the absence of correlation between optical pulses, the net sample-magnetization lies on the magnetic field axis; the transverse component vanishes in the average. The weak-light restriction means here that the equi-

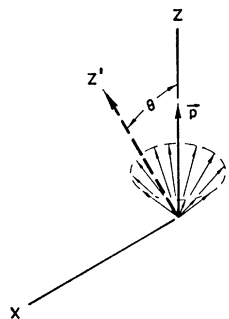


FIG. 4. In a pulse approximation, the off-axis light beam creates increments of polarization on the z axis which precess about the magnetic field in a cone whose net polarization \mathbf{p} is parallel to the magnetic field.

¹⁸ If, instead, the fractional increase in total angular momentum were the observed quantity, the change of sign in Eq. (6) would be ignored in calculating Eq. (14), giving $[(7F_+^2-1)/9F_+^3]$, which does approach zero in the limit of large I .

¹⁹ P. A. Franken, Phys. Rev. **121**, 508 (1961).

²⁰ W. E. Bell, A. L. Bloom, and J. Lynch, Rev. Sci. Instr. **32**, 688 (1961).

rium magnetization is never large enough to affect this process significantly. The relaxation processes are defined in the usual way in the magnetic field's coordinate system. The new equilibrium polarization is

$$P_z^0 = P_e^0 \cos\theta. \quad (15)$$

MAGNETIC RESONANCE

A circularly polarized rf magnetic field (e.g., $H_x = H_1 \cos\omega t$, $H_y = -H_1 \sin\omega t$) in the plane perpendicular to the static magnetic field H_0 can reorient the electron polarization. Bloch's phenomenological equations^{21,10} describe the motion of the magnetic moment vector through its components $M_z = \gamma\hbar F_+NP_z$, etc. The projection of the electron polarization on the optical axis is then

$$P_{z'} = P_z \cos\theta + P_x \sin\theta, \quad (16)$$

where the optical z' axis is arbitrarily taken to be in the x - z plane.

If the time dependence is made explicit, the steady-state solutions will have the form

$$\begin{aligned} P_z &= P_z^0 g_z(\omega), \\ P_x &= P_z^0 g_1(\omega) \sin(\omega t - \phi), \\ P_y &= P_z^0 g_1(\omega) \cos(\omega t - \phi). \end{aligned} \quad (17)$$

For small magnetic fields, where the Zeeman resonance lines are completely unresolved, the steady-state solutions of Bloch's equations apply directly that

$$\begin{aligned} g_z(\omega) &= \frac{1 + (\Delta\omega T_2)^2}{1 + (\Delta\omega T_2)^2 + (\gamma H_1)^2 T_1 T_2}, \\ g_1(\omega) &= \frac{\gamma H_1 T_2 [1 + (\Delta\omega T_2)^2]^{1/2}}{1 + (\Delta\omega T_2)^2 + (\gamma H_1)^2 T_1 T_2}. \end{aligned} \quad (18)$$

T_1 is the longitudinal relaxation time already introduced, T_2 is the "transverse relaxation time" characterizing the loss of phase memory, and

$$\Delta\omega = \omega - \gamma H_0, \quad \tan\phi = \Delta\omega T_2.$$

In practice, a linearly polarized rf field ($H_x = 2H_1 \cos\omega t$, $H_y = 0$) was used without measureable error.²²

For resolved ground-state lines, the effective polarization reoriented in a single resonance between sublevels m_k and m_{k-1} is $(\epsilon_k^0 - \epsilon_{k-1}^0)/F_+$, which is a fraction

$$\frac{3}{2F_+} \left[\frac{2F_+ \pm (F_+^2 - 1)}{2F_+^4 + (5F_+^2 - 1)} \right]$$

of the total electron polarization of the vapor. Since only two levels are involved ("fictitious spin $\frac{1}{2}$ "^{23,24}), the

²¹ F. Bloch, Phys. Rev. **70**, 460 (1946).

²² F. Bloch and A. Siegert, Phys. Rev. **57**, 522 (1940).

²³ A. Abragam, *The Principles of Nuclear Magnetism* (Oxford University Press, London, 1961).

²⁴ R. P. Feynman, E. L. Vernon, Jr., and W. R. Hellwarth, J. Appl. Phys. **28**, 49 (1957).

steady-state solutions above must be corrected by replacing γH_1 by $[(F_k + m_k)(F_k - m_k + 1)]^{1/2} \gamma H_1$.

Then the absorption rate per atom can finally be written

$$\beta = \beta_0(1 - P_{z'}) = \beta_0 \{ 1 - \beta_0 T_1 \zeta [\cos^2 \theta g_z(\omega) + \sin \theta \cos \theta g_1(\omega) \sin(\omega t - \phi)] \}. \quad (19)$$

The time-independent term is the one usually used in transmission-monitored optical-pumping experiments. The time-dependent term was of primary interest in this experiment. In particular, if the source of H_1 current is removed and the rf current $i(\omega)$ from the photocell is fed back to the H_1 coil through amplifiers of fixed gain A and suitable phase shift α , stable oscillations develop whose frequency is controlled by the rubidium transition.

From the definition of H_x , steady-state operation requires

$$2H_1 \cos \omega t = A i(\omega),$$

where the "gain" A is taken to include all the engineering parameters of the feedback loop. This imposes a condition on the phase:

$$\cos \omega t = \sin(\omega t - \phi + \alpha) \quad (20)$$

and a condition on the gain

$$2H_1 = AN\beta_0^2 T_1 \zeta g_1(\omega) \cos \theta \sin \theta. \quad (21)$$

But $g_1(\omega)$ is a function of H_1 . Solving for H_1 in the weak-field case above,

$$H_1 = [AN\beta_0^2 \zeta \cos \theta \sin \theta - (1/\gamma^2 T_1 T_2)]^{1/2}, \quad (22)$$

which implies a threshold of oscillation when the expression under the radical is zero. (For resolved lines, again, γ and N must be modified.)

This oscillator differs from the conventional maser only in the means of detection and the use of external gain and phase shift. Like a maser, the frequency-determining element is saturable and operation beyond saturation is unstable.²⁵ In general, higher order transitions not described by this theory further complicate the behavior beyond saturation. In our case, the gain was adjusted for maximum stability.

By the definition of ϕ , following Eq. (18), the phase condition implies a frequency requirement

$$\omega_{\text{osc}} = (1/T_2)(\alpha - \pi/2) + \gamma H_0. \quad (23)$$

In practice the first term is set to zero as nearly as possible by maximizing the amplitude for small gain.

Variations in loop phase shift of α can arise in many ways, causing frequency noise or failure to follow the magnetic field H_0 . For example, the H_0 axis and optical axis have been taken here as defining the x - z plane, with the H_1 field introduced on the x axis. Small changes in H_0 direction rotate the x - z plane away from the H_1 coil, changing α . To prevent such phase shifts, the axis of the H_1 coil was made parallel to the light beam.⁷

²⁵ W. E. Lamb, Jr., Phys. Rev. 134, A1429 (1964).

THE STARK EFFECT

Postulating a permanent electric dipole moment p for the atom and taking the applied electric field to be parallel to the magnetic field (defining the z axis), the perturbing Hamiltonian is $-\mathbf{p} \cdot \mathcal{E} = -eD\mathcal{E} \cos \theta$. The length $D = p/e$ is customarily used to express the magnitude of the moment and is analogous to the magnetic dipole convention, so that the linear shift in Zeeman frequency is

$$\delta\nu(\mathcal{E}) = eD\mathcal{E}/hF. \quad (24)$$

Even in the absence of a new linear Stark effect, the Zeeman sublevels are depressed by the usual quadratic Stark shift $W_{F,m}$, but the shift in frequency

$$\delta\nu = (1/h)(W_{F,m} - W_{F,m-1}) \quad (25)$$

is very small. Intuitively, the nuclear electric quadrupole moment should be expected to contribute to the frequency shift by interaction with the fraction of $5^2P_{3/2}$ state admixed in the first-order perturbed wave function. In fact, the magnetic hyperfine energy is also coupled to the ground state in an m -dependent way. The significant contributions to $W_{F,m}$ are then

$$W_{F,m} = e^2 \mathcal{E}^2 \sum_{J,F'} \frac{|\langle 5^2S_{1/2}, F, m | z | 5^2P, J, F', m \rangle|^2}{(\Delta W)^2} \times \langle 5^2P, J, F', m | \text{hfs} | 5^2P, J, F', m \rangle, \quad (26)$$

where ΔW is the optical D -line energy separation and only the $5P$ state is included in the sum because of its oscillator strength. The corresponding fine-structure term does not appear because the sum $\sum_{F'} |\langle 5^2S_{1/2}, F, m | z | 5^2P, J, F', m \rangle|^2$ is independent of m by "spectroscopic-stability" arguments. The sum in Eq. (26) has been performed by Lipworth and Sandars² (the result appears in third order if the hyperfine interaction is treated as a perturbation; the derivation here corresponds to a second-order energy calculation, of course, and can be obtained, e.g., by expanding the energy

FIG. 5. An ($F=3, m_F=-3 \leftrightarrow -2$) transition and ($F=3, m_F=-2 \leftrightarrow -1$) transition partly resolved. This display was made by synthesizing an rf frequency which followed magnetic-field fluctuations corresponding to hundreds of linewidths.



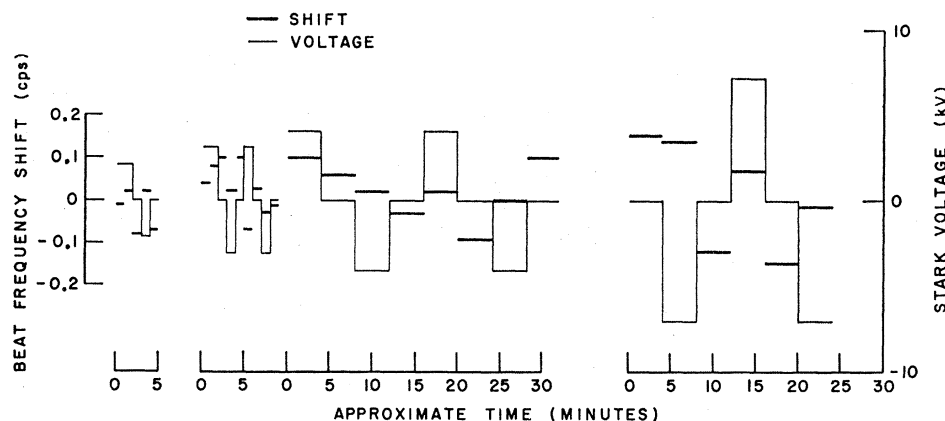


FIG. 6. The heavy lines indicate the measured frequency shift and the period over which it was averaged. The applied voltage is represented by light lines for the scale at right.

denominators).²⁶ For the transition ($F=3, m_F=+3$) \leftrightarrow ($F=3, m_F=+2$),

$$\delta\nu(\mathcal{E}^2) = + \frac{3(\alpha\mathcal{E}^2)}{4(\Delta W)} \left(\frac{3IA_{3/2} - 2b_{3/2}}{2I+1} \right) \quad (27)$$

for Rb⁸⁵, $I = \frac{5}{2}$; $\Delta W = 2.5 \times 10^{-12}$ erg; the magnetic hyperfine interaction constant in the $5^2P_{3/2}$ state²⁷ is $A_{3/2} = 25.3$ Mc/sec; the electric quadrupole constant in the $5^2P_{3/2}$ state²⁸ is $b_{3/2} = 24.4$ Mc/sec; the electric field \mathcal{E} is in esu; and α , the measured electric polarizability in rubidium,²⁸ is 40×10^{-24} cm³. The resulting shift is 0.31×10^{-8} \mathcal{E}^2 cps (\mathcal{E} is V/cm) and was too small to be observed in this experiment.

RESULTS

With the two Rb oscillators running at about 210 kc/sec, and with the gradient adjusted for the sample on the west to operate about 300 to 400 cps higher than that toward the east, the typical minimum random uncertainty in beat frequency, which under favorable conditions was of the order of 0.1 cps, set the limit to the sensitivity for measurement of frequency shifts between these two oscillators. This is equivalent to a shift in magnetic field of 2×10^{-7} G.

The longitudinal relaxation time T_1 of the absorption cells were about 1/10 sec. Reducing the area of the aperture in the absorption cell wall from about 3/7 mm² to about 1/9 mm² failed to increase T_1 . (These times were measured by saturating the magnetic-resonance lines and then observing the initial slope of the photocurrent as a function of light intensity.) Since the field fluctuations were many times as large as the magnetic-resonance width, the line shape was examined with the aid of an H_1 field whose frequency was generated by a crude synthesizer from the photocurrent of the neighboring rubidium oscillator. The synthesizer permitted the addition of a small frequency increment to sweep across part of the line. The top of a typical $m_k = +3$ to

+2 transition and its first neighbor are shown in Fig. 5. This was the peak on which the oscillators ran. The quadratic Zeeman splitting separates the centers of these lines by about 30 cps. Neither resolved lines nor the weak-light limit were fully realized here.

Any change in Stark voltages across the absorption cell were followed by fluctuations in photocurrent which diminished over a time of the order of a minute. This slow return to equilibrium seemed related to the wall coating. The only attempt with 60-cps Stark fields damaged the coating in the cell and indicated that the ability of the lining to withstand strong electric fields may have been greater at dc. When Stark voltages were very gradually raised to the chosen value, spurious effects were small and disappeared when the voltage was fixed.

No Stark effect was observed (Fig. 6). With electric fields of 10 kV across the 25 mm of sample length, small, apparently reproducible shifts were seen, some dependent on field polarity. They were judged spurious because correlation existed between the size of the shifts and the history of previous applications of the field (although no evidence of internal discharge was visible to the dark-adapted eye or detectable in sample pressure). Thus data taken for the higher voltages were discarded.

Fields of ± 7000 V across 25 mm of sample taken with the frequency uncertainty of about ± 0.1 cps implies, through Eq. (24), that if a linear electric dipole exists, then its length D must be less than 0.7×10^{-18} cm.

ACKNOWLEDGMENTS

I wish to express my thanks to Professor H. G. Dehmelt who suggested this work, to Jake Jonson, who built the titanium pump electrode structure and did all the glass work, and to Dr. G. S. Hayne for helpful discussions about the calculations.

APPENDIX

The sums $\sum_j B_{jk}$ and $\sum_j B_{kj}$ were derived by simply taking the implied matrix products of absorption

²⁶ R. D. Haun and J. R. Zacharias, Phys. Rev. **107**, 107 (1957).

²⁷ B. Senitzky and I. Rabi, Phys. Rev. **103**, 315 (1956).

²⁸ G. E. Chamberlain and J. Zorn, Phys. Rev. **129**, 677 (1963).

TABLE I. Unnormalized absorption probabilities $P_{\alpha k}$ in terms of initial-state quantum numbers.

Final $^2P_{1/2}$ state sublevels α	Initial $^2S_{1/2}$ state sublevels k	F_+, m	$F_+ - 1, m$
$F_+, m+1$	$F_+, m+1$	$\frac{1}{2}(F_+ - m)(F_+ + m + 1)$	$\frac{1}{2}(F_+ + m)(F_+ + m + 1)$
$F_+ - 1, m+1$	$F_+ - 1, m+1$	$\frac{1}{2}(F_+ - m)(F_+ - m - 1)$	$\frac{1}{2}(F_+ + m)(F_+ - m - 1)$

probabilities $P_{\alpha k}$ and spontaneous emission probabilities $Q_{j\alpha}$ calculated from electric dipole matrix elements with angular-momentum wave functions.²⁹ The sum $\sum_j B_{jk} = \sum_{j\alpha} Q_{j\alpha} P_{\alpha k} = \sum_{\alpha} (\sum_j Q_{j\alpha}) P_{\alpha k}$ is easily performed because $\sum_j Q_{j\alpha}$ must be independent of the initial excited sublevel α . Then using Table I, $\sum_j B_{jk} \propto \sum_{\alpha} P_{\alpha k} \propto F_+(F_+ \mp M) \propto 1 \mp (M/F_+)$. A normalization

 TABLE II. Unnormalized spontaneous-emission probabilities $Q_{k\alpha}$ in terms of final-state quantum numbers.

Final $^2S_{1/2}$ state sublevel k	Initial $^2P_{1/2}$ state sublevels α	$F_+, m+1$	F_+, m	$F_+, m-1$
F_+, m	F_+, m	$(F_+ + m + 1)(F_+ - m)$	$2m^2$	$(F_+ - m + 1)(F_+ + m)$
$F_+ - 1, m$	$F_+ - 1, m$	$(F_+ + m + 1)(F_+ + m)$	$2(F_+^2 - m^2)$	$(F_+ - m + 1)(F_+ - m)$
	$F_+ - 1, m+1$	$F_+ - 1, m+1$	$F_+ - 1, m$	$F_+ - 1, m-1$
F_+, m	$F_+ - 1, m$	$(F_+ - m - 1)(F_+ - m)$	$2(F_+^2 - m^2)$	$(F_+ + m - 1)(F_+ + m)$
$F_+ - 1, m$	$F_+ - 1, m$	$(F_+ - m - 1)(F_+ + m)$	$2m^2$	$(F_+ + m - 1)(F_+ - m)$

 TABLE III. Unnormalized absorption probabilities $P_{\alpha j}$ in terms of final-state quantum numbers in Table II.

Final $^2P_{1/2}$ state sublevels α	Initial $^2S_{1/2}$ state sublevels j	F_+, m	$F_+, m-1$	$F_+, m-2$
$F_+, m+1$	$F_+, m+1$	$(F_+ + m + 1)(F_+ - m)$	$(F_+ - m + 1)(F_+ + m)$	$(F_+ - m + 1)(F_+ + m - 1)$
F_+, m	F_+, m			
$F_+, m-1$	$F_+, m-1$			
$F_+ - 1, m+1$	$F_+ - 1, m+1$	$(F_+ - m - 1)(F_+ - m)$	$(F_+ - m + 1)(F_+ - m)$	$(F_+ - m + 1)(F_+ - m + 1)$
$F_+ - 1, m$	$F_+ - 1, m$			
$F_+ - 1, m-1$	$F_+ - 1, m-1$			
	$F_+ - 1, m$	$F_+ - 1, m$	$F_+ - 1, m-1$	$F_+ - 1, m-2$
$F_+, m+1$	$F_+, m+1$	$(F_+ + m + 1)(F_+ + m)$	$(F_+ + m - 1)(F_+ + m)$	$(F_+ + m - 1)(F_+ + m - 1)$
F_+, m	F_+, m			
$F_+, m-1$	$F_+, m-1$			
$F_+ - 1, m+1$	$F_+ - 1, m+1$	$(F_+ - m - 1)(F_+ + m)$	$(F_+ + m - 1)(F_+ - m)$	$(F_+ - m + 1)(F_+ + m - 1)$
$F_+ - 1, m$	$F_+ - 1, m$			
$F_+ - 1, m-1$	$F_+ - 1, m-1$			

constant A can be evaluated by Eq. (2):

$$\begin{aligned} \sum_{jk} B_{jk} &= 4F_+ = A \sum_m 1 \mp \frac{m}{F_+} \\ &= A[(2F_+ + 1) + (2F_+ - 1)] = A[4F_+]; \end{aligned}$$

so $A=1$ and $\sum_j B_{jk} = 1 \mp (m/F_+)$, where the upper sign implies an initial state (F_+, m) and lower sign, initial state $(F_+ - 1, m)$. For the sum $\sum_j B_{kj} = \sum_{j\alpha} Q_{k\alpha} P_{\alpha j} = \sum_{\alpha} Q_{k\alpha} [\sum_j P_{\alpha j}]$, the probabilities for all transitions ending in the final-state sublevel k must be written in

terms of the quantum numbers for that state $(F_+, m$ or $F_+ - 1, m)$ as shown in Tables II and III.

Collecting terms:

$$\sum_{\alpha} Q_{k\alpha} \sum_j P_{\alpha j} \propto \begin{pmatrix} 3F_+^3 + (-F_+^2 + 4F_+ - 2)m \\ 3F_+^3 + (F_+^2 + 4F_+ + 2)m \end{pmatrix}.$$

Normalizing as before:

$$\sum_{jk} B_{kj} = 4F_+, \quad \sum_j B_{kj} = 1 + \left[\frac{4F_+ \mp (F_+^2 + 2)}{3F_+^3} \right] m_k.$$

²⁹ E. U. Condon and A. G. Shortley, *The Theory of Atomic Spectra* (Cambridge University Press, London, 1935).